ÖHÜ Müh. Bilim. Derg. / OHU J. Eng. Sci.

ISSN: 2564-6605

Ömer Halisdemir Üniversitesi Mühendislik Bilimleri Dergisi, Cilt 6, Sayı 2, (2017), 737-751
Omer Halisdemir University Journal of Engineering Sciences, Volume 6, Issue 2, (2017), 737-751

Araştırma / Research

EFFECT OF ANISOTROPY DETERMINATION METHODS ON FORMING LIMIT CURVE PREDICTION OF 304L STAINLESS STEEL

Serkan TOROS (ORCID: 0000-0003-0438-2862)*

Makine Mühendisliği Bölümü, Mühendislik Fakültesi, Niğde Ömer Halisdemir Üniversitesi, Niğde, Türkiye

Geliş / Received: *21.04.2017*
Düzeltmelerin gelişi / Received in revised form: *02.06.2017*
Kabul / Accepted: *03.06.2017*

ABSTRACT

In recent years, numerous researchers have focused on the determination of the formability limits of the sheet materials experimentally and numerically. Due to some troubles encountered during the experimental studies, the modeling of the formability characteristics of the materials via simple experiments like tensile tests is the main issue for the most researchers. In the literature, most of the developed model results strongly depend on yield functions used and their parameters which reflect the materials' anisotropic behaviors. In this study, the capability of BBC family yield functions (BBC2000, 2003, 2005 and 2008) are investigated to construct the forming limit diagram of 304L stainless steel by using the Marciniak-Kuczynski instability model. The models are evaluated for different anisotropy determination approaches and the predicted results have been compared with the experimental forming limit diagram.

Keywords: 304L, forming limit diagram, BBC family, Marciniak-Kuczynski model

304L PASLANMAZ ÇELİĞİN ŞEKİLLENDİRME SINIR DİYAGRAMININ BELİRLENMESİNDE ANİZOTROPİ BELİRLEME METODUNUN ETKİSİ

ÖZ

Son yıllarda birçok araştırmacı sac malzemelerin şekillendirme sınırlarının deneysel ve nümerik olarak belirlenmesi üzerine odaklanmışlardır. Deneysel çalışmalar esnasında birçok zorluklarla karşılaşılmasından ötürü, birçok araştırmacı için malzemelerin şekillendirme karakteristiklerini çekme deneyi gibi basit deneylerden modellenerek elde edilmesi temel bir mesele haline gelmiştir. Literatürde geliştirilen birçok model sonucu kullanılan akma yüzey fonksiyonlarına ve malzemelerin anizotropik davranışlarını yansıtan model parametrelerine büyük ölçüde bağlı bulunmaktadır. Bu çalışma kapsamında BBC ailesi (BBC2000, 2003, 2005 ve 2008) akma yüzeyleri Marciniak-Kuczynski kararsızlık modeli ile 304L paslanmaz çeliğin şekillendirme sınır diyagramının oluşturulması noktasında kullanılmıştır. Modeller farklı anizotropi belirleme yöntemleri için değerlendirilmiş ve tahmin edilen sonuçlar deneysel sonuçlarla karşılaştırılmıştır.

Anahtar Kelimeler: 304L, şekillendirme sınır diyagramı, BBC ailesi, Marciniak–Kuczynski modeli

1. INTRODUCTION

One of the most frequently used materials in the sheet metal industry is the stainless steels which have the high corrosion resistance, good weldability and formability characteristics. Since they have relatively low yield strength, they seem to be less appropriate for structural applications but are widely employed in the

*Corresponding author / Sorumlu yazar. Tel.: +90 388 225 2355; e-mail / e-posta: serkantoros@ohu.edu.tr

transportation, nuclear, aerospace and fuel cell technology industries.

For a successful application of any material, the formability limitations need to be determined. In order to carry out the forming operation of the sheet metals faultlessly, a diagram namely **F**orming **L**imit **D**iagram (FLD) is used in which the safe, critical and failure deformation regions are indicated. In sheet metal industry and studies, it is widely used and considered as one of the substantial tools to comprehend the formability characteristics of sheet metals under various stamping conditions. Every sheet metal has its own forming limit curve which controls its formability, strain limit and critical regions under various deformation modes. The forming limit diagram was discovered by Keeler and Backhofen [1], and Goodwin [2] provided a useful experimental measure of stamping harshness in the absence of any significant failure.

At the beginning of the constructing of the theoretical approaches for predicting the formability limits, Swift[3] and Hill [4] developed instability criteria. Swift [3] developed diffuse necking theory for a biaxially loaded element, which is based on the maximum force theory. The right hand side (RHS) of the FLD, where both major and minor strains are positive, can be determined via this model. Then, Hill [4] proposed the localized necking phenomenon which predicts the deformation modes at the left hand side (LHS) of the FLD where the localized neck develops along the zero elongation direction. When these diffuse and localized necking theories are used together, the whole FLD can be constructed for all straining modes which vary with uniaxial to biaxial conditions. Other theoretical approaches to determine the localized necking during the stamping operation are bifurcation theory [5], perturbation theory [6] and the shear instability criterion [7]. Another most commonly used instability criteria for the determination of FLD is the Marciniak-Kuczynski (M-K) model [8]. In the model, it is assumed that there is an imperfection on the material due to the applied rolling operation prior to the forming operation. The derivation of the model formulation and its parameters are conducted to the force balance equilibrium for the both groove and normal regions. Hutchinson and Neale [9] then extended the M-K model to tension-comparison condition and the assumed groove direction on the sheet metal is not perpendicular to the loading direction. Therefore, the strain components need to be recalculated for all different directions. The minimum groupings of major and minor strains are then selected for each deformation mode and groove angle.

As aforementioned before, one of the most important tools used for the calculation of the stress and strain components on the materials is the yield functions. In the literature, there are several investigations about the prediction of the forming limits via various instability criteria and anisotropic yield functions. Since sheet materials show anisotropic behavior because of its manufacturing nature, anisotropic yield functions should be employed in the models to determine the plastic strain increments during the calculation of the limit strains. To predict the FLD under a linear strain path, Banabic et al.[10] focused on a comparison of different modeling approaches. In the study, orthotropic yield criterion developed by BBC2003 [11] was considered for four models, namely Marciniak-Kuczynski model, the modified maximum force criterion (MMFC) according to Hora [12], Swift's diffuse [3] and Hill's localized necking approach [4]. Arrieux [13] studied on the prediction of the onset of necking in deep drawing process by using a numerical method. In the analysis, the forming limit stress surface of a sheet metal was determined based on M-K model. A comparative study to predict the FLD was also presented by Slota and Spisak [14]. Three mathematical models (M-K model, Hill-Swift model and Sing-Rao model) as well as the empirical model by the NADDRG were investigated and their results were compared with the experimental results. The M-K model provides better agreement with experimental results when compared to the other considered models.

In this study, the forming limit characteristics of 304L stainless steel are investigated via M-K model. Additionally, in the model BBC family anisotropic yield functions (BBC2000, BBC2003, BBC2005 and BBC2008) are evaluated in order to compare the applicability.

2. MATERIAL AND METHODS

The uniaxial tensile tests were applied to 1.3 mm thick sheet samples which are prepared according to the ASTM E8 [15] standard at different strain rate (0.0016, 0.042, 0.33 s^{-1}) in order to determine the mechanical properties such as anisotropies and yield stresses which are used for calculating the yield surface and FLD models. All tests were executed on a Shimadzu Autograph 100 kN tensile testing machine. Material deformation was measured with a non-contact video type extensometer measurement system. Each test was repeated at least three times and their average was used in flow stress–strain curves.

2.1. Flow Curves and Their Features at Different Strain Rates

Figure 1 indicates the tensile characteristics of the 304L stainless steel with respect to the different directions at selected deformation speeds. As can be seen from the figure, the yield strength and maximum tensile strength of

the material are different for different directions and deformation speeds. The studied austenitic stainless steel shows TRIP (**TR**ansformation **I**nduced **P**lasticity) and/or TWIP (**TW**ining **I**nduced **P**lasticity) effect which contributes to the plastic deformation ability of the materials. This contribution is directly related with the process parameters like the temperature, the strain rate and the loading type. Therefore, the material response at different strain rates might be significantly different in terms of the strength and the elongation.

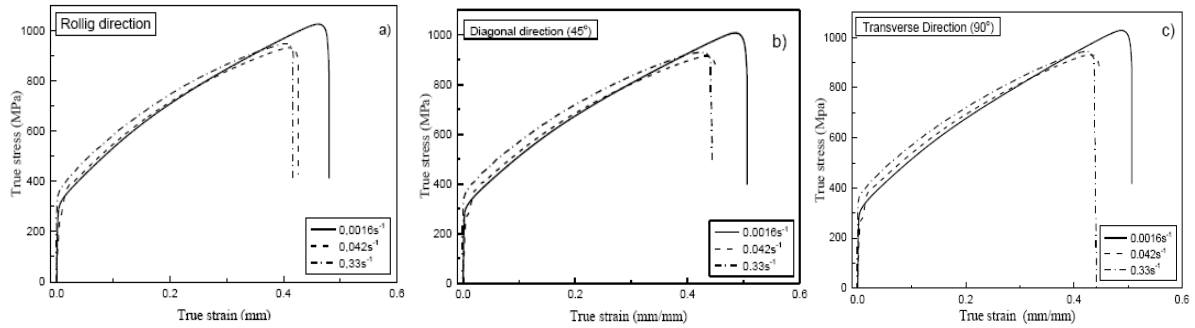

Figure 1. Tensile properties of 304L stainless steel along with various directions under different strain rates.

The critical stress levels like yield and ultimate tensile strengths are determined from the engineering stress-strain curve and plotted in Figure 2 for each strain rates and orientations. It is seen that the yield strength of the material increases with increasing the strain rate however the uniform elongation tends to decrease. In addition, the ultimate tensile strength does not have a simple behavior because of a special mechanism that occurs with the given deformation. Since the austenitic stainless steels are consisting of the unstable austenite phases, the martensitic transformation mechanism occurs with the plastic deformation in the microstructure. Therefore, the decreasing rate of the work hardening is much slower. This phenomena cause to delaying of the necking, revealing that the higher formability can be obtained. This transformation mechanism which affects the general mechanical response of the materials like elongation, hardening and strength, is influenced by the strain rate which decreases the martensitic transformation [16]. As depicted in Figure 2c, the slow tensile test has a higher tensile strength with respect to martensitic transformation.

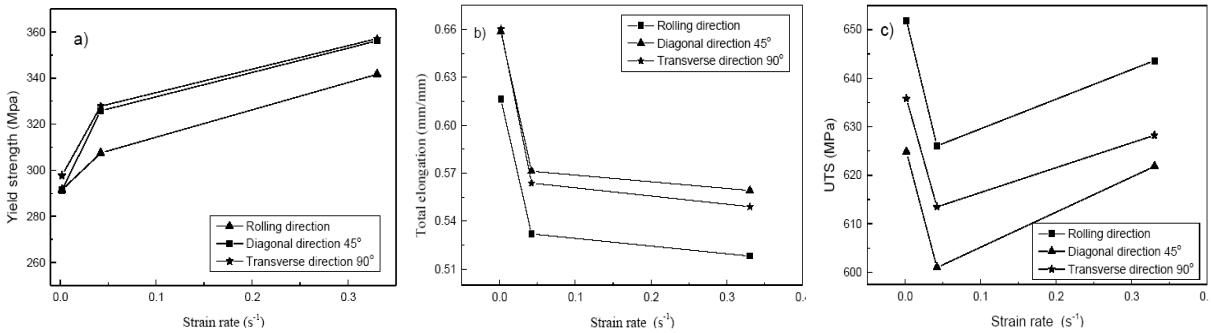

Figure 2. Variation of the mechanical properties of the 304L stainless steel with strain rates

In the study, besides the general mechanical responses, the anisotropic coefficients (Lankford's parameters) of the material were also calculated at specified orientations and deformation speeds. Two different strain levels (15-20%) were also taken into considerations since the martensitic transformation has occurred during the plastic deformation. In addition to this, the anisotropy values were also calculated by using the slope of the strain values (width and longitudinal) via the equation given below [17]:

$$r_{\varphi} = -\left(\frac{\frac{\varepsilon_w}{\varepsilon_l}}{1+\frac{\varepsilon_w}{\varepsilon_l}} \right) \tag{1}$$

The variation of the longitudinal strains with respect to the width strains were plotted with their linear fit in

Figure 3. The calculated slopes are then replaced to $\varepsilon_w/\varepsilon_l$ in the Equation 1 for each orientation and strain rate. All calculated results for the anisotropies are listed in Table 1 for each situation.

Table 1. Yield stress and Lankford parameters of the 304L stainless steel

	R-value (%15)			R-value (%20)			R-value (Slope)		
Strain rate (s^{-1}) / Direction	**0.0016**	**0.042**	**0.33**	**0.0016**	**0.042**	**0.33**	**0.0016**	**0.042**	**0.33**
Rolling direction (RD)	0.866	0.894	0.541	0.619	0.743	0.784	0.672	0.776	0.706
Diagonal direction (DD)	1.08	1.036	1.018	1.029	1.060	1.006	1.036	1.049	1.008
Transverse direction (TD)	0.907	0.793	0.855	0.863	0.861	0.829	0.680	0.841	0.834

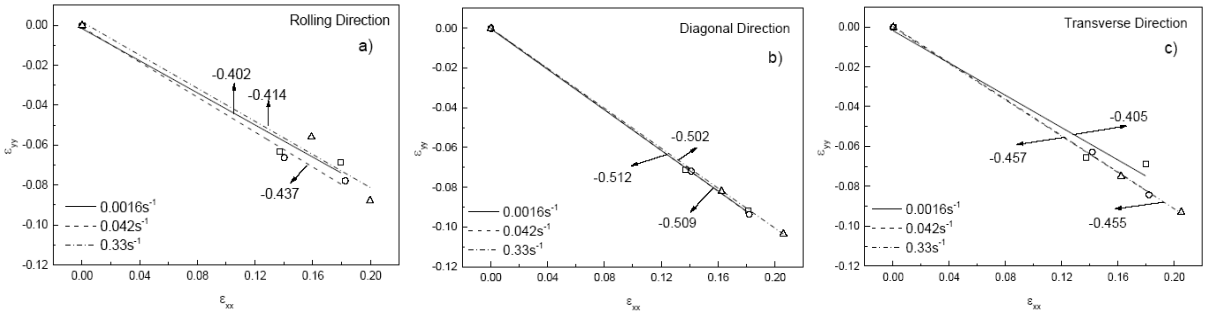

Figure 3. Calculation of the anisotropies via the slope methodology

2.2. Yield Functions

2.2.1. BBC-2000

One of the most widely used yield function in the literature is the BBC-2000 anisotropic yield criterion which is the first derived formulation of the Banabic et al. [18] from Barlat and Lian's yield function [19] for orthotropic sheet metals under plane stress conditions. In the model, two additional material parameters *b* and *c* are added as a multiplier of the stress definitions to provide a better prediction of the material behavior. The equivalent form of the criterion is given below:

$$\bar{\sigma} = \left[a\left(b\tau + c\psi\right)^{2k} + a\left(b\tau - c\psi\right)^{2k} + \left(1-a\right)\left(2c\psi\right)^{2k} \right]^{\frac{1}{2k}} \tag{2}$$

where, a, b, c and k are the material parameters which are used to fit the function to the experimental data. The exponent k is associated with the crystal structure of the sheet material (3 and 4 for BBC and FCC metals, respectively) whereas τ and ψ are the functions of the stress components which can be described as:

$$\begin{aligned} \tau &= M\sigma_{11} + N\sigma_{22} \\ \psi &= \sqrt{\left(P\sigma_{11} + Q\sigma_{22}\right)^2 + R\sigma_{12}^2} \end{aligned} \tag{3}$$

2.2.2. BBC-2003

Another plane stress yield criterion is proposed by Banabic et al. [20] accounting for biaxial deformation mode of the materials. The precision capability of the model can be improved by this additional mechanical parameter:

$$\bar{\sigma} = \left[a\left(\tau + \psi\right)^{2k} + a\left(\tau - \psi\right)^{2k} + \left(1-a\right)\left(2\Lambda\right)^{2k} \right]^{\frac{1}{2k}} \tag{4}$$

In the above equation, a is the material parameter like in the previous yield criterion, and τ, ψ and Λ are the composition of the planar stress tensor components defined as:

$$\begin{aligned}\tau &= \frac{\sigma_{11} + M\sigma_{22}}{2} \\ \psi &= \sqrt{\left(\frac{N\sigma_{11} - P\sigma_{22}}{2}\right)^2 + Q^2\sigma_{12}\sigma_{21}} \\ \Lambda &= \sqrt{\left(\frac{R\sigma_{11} - S\sigma_{22}}{2}\right)^2 + T^2\sigma_{12}\sigma_{21}}\end{aligned} \tag{5}$$

2.2.3. BBC-2005

Similar to the BBC2003, the author proposed a new formulation of the yield stress with additional material parameters. The equivalent stress form the yield function is given by the following formula;

$$\bar{\sigma} = \left[a\left(\Lambda + \Gamma\right)^{2k} + a\left(\Lambda - \Gamma\right)^{2k} + b\left(\Lambda + \Psi\right)^{2k} + b\left(\Lambda - \Psi\right)^{2k} \right]^{\frac{1}{2k}} \tag{6}$$

where

$$\begin{aligned}\Gamma &= L\sigma_{11} + M\sigma_{22} \\ \Lambda &= \sqrt{\left(N\sigma_{11} - P\sigma_{22}\right)^2 + \sigma_{12}\sigma_{21}} \\ \psi &= \sqrt{\left(Q\sigma_{11} - R\sigma_{22}\right)^2 + \sigma_{12}\sigma_{21}}\end{aligned} \tag{7}$$

In Equation (7), L, M, N, P, Q and R are also material parameters that need to be calculated by using the Lankford parameters and yield stresses with respect to the material orientations.

2.2.4. BBC-2008

In order to enhance the representability of BBC2005 [21] yield criterion, another flexible model is proposed by the Banabic et al. [22]. This model can be expressed as a finite series whose limitation is depended on the experimental data obtained for different orientations. The equivalent stress can be expressed as:

$$\frac{\bar{\sigma}^{2k}}{w-1} = \sum_{i=1}^{s}\left\{ w^{i-1}\left\{\left[L^i + M^i\right]^{2k} + \left[L^i - M^i\right]^{2k}\right\} + w^{s-i}\left\{\left[M^i + N^i\right]^{2k} + \left[M^i - N^i\right]^{2k}\right\}\right\} \tag{8}$$

$$k, s \in N^* \quad w = \left(3/2\right)^{\frac{1}{s}} > 1$$

$$\begin{aligned}L^i &= l_1^i\sigma_{11} + l_2^i\sigma_{22} \\ M^i &= \sqrt{\left[m_1^i\sigma_{11} - m_2^i\sigma_{22}\right]^2 + \left[m_3^i(\sigma_{11} - \sigma_{22})\right]^2} \\ N^i &= \sqrt{\left[n_1^i\sigma_{11} - n_2^i\sigma_{22}\right]^2 + \left[n_3^i(\sigma_{11} - \sigma_{22})\right]^2}\end{aligned} \tag{9}$$

$l_1^i, l_2^i, m_1^i, m_2^i, m_3^i, n_1^i, n_2^i, n_3^i$ are all the material parameters. In the model, it is possible to extend the equivalent stress function with respect to the obtained experimental materials parameters. For example; s can be taken as 1 for only 6 material parameters ($\sigma_0^{\exp}, \sigma_{45}^{\exp}, \sigma_{90}^{\exp}, r_0^{\exp}, r_{45}^{\exp}, r_{90}^{\exp}$).

It is also possible to open finite series for $s=2$ and $s=3$ for the same number of material parameters. However, this form of the yield function can cause to the over-estimate situation in the mathematical expression. Therefore, more experimental results like $\sigma_0^{exp},\sigma_{15}^{exp},\sigma_{30}^{exp},\sigma_{45}^{exp},\sigma_{60}^{exp},\sigma_{75}^{exp},\sigma_{90}^{exp},\sigma_b^{exp},r_0^{exp},r_{15}^{exp},r_{30}^{exp},r_{45}^{exp},r_{60}^{exp},r_{75}^{exp},r_{90}^{exp},r_b^{exp}$ are required for the $s>1$ values.

2.3. Material Parameter Identification via Optimization Procedure

In the current study, the anisotropy parameters of the models were determined by applying well-known least square method and the following error function ε in order to increase the accuracy of the yield criteria:

$$\varepsilon(parameters)=\sum_{i=1}^{k}\left(\frac{Y_{\varphi i}-\sigma_{\varphi i}^{\exp}}{\sigma_{\varphi i}^{\exp}}\right)^2+\sum_{i=1}^{k}\left(\frac{\bar{r}_{\varphi i}-\bar{r}_{\varphi i}^{\exp}}{\bar{r}_{\varphi i}^{\exp}}\right)^2=Min \tag{10}$$

In Equation (10), φi shows the orientation angle with respect to the original rolling direction of the specimen, while $Y_{\varphi i}$ and $\bar{r}_{\varphi i}$ are the calculated results of yield stress (Equation 16) and anisotropy (Equation 17), respectively. $\sigma_{\varphi i}^{\exp}$ and $\bar{r}_{\varphi i}^{\exp}$,on the other hand, are the experimental results for the yield stress and the anisotropy, respectively.

In order to calculate the variation of the yield stresses, the tensor transformation rule is employed. The stress components in a tensile test specimen can be given for the different orientation angles as:

$$\sigma_{11}=Y_{\varphi}.\cos^2\varphi \tag{11}$$

$$\sigma_{22}=Y_{\varphi}.\sin^2\varphi \tag{12}$$

$$\sigma_{12}=Y_{\varphi}.\cos\varphi.\sin\varphi \tag{13}$$

By replacing Equations (11-13) into the relationship defining the equivalent stress for each yield criteria and taking into account its homogeneity, we can obtain:

$$\bar{\sigma}=Y_{\varphi}F_{\varphi} \tag{14}$$

where Y_{φ} is the calculated yield stress with respect to the orientation angles like 0º, 45º, 90º and F_{φ} is a function depending the angle φ. The variation of the yield stresses and anisotropies with respect to the angle φ can be calculated by using Equations (15) and (16), respectively.

$$Y_{\varphi}=\frac{\bar{\sigma}}{F_{\varphi}} \tag{15}$$

$$\bar{r}_{\varphi}=\frac{\bar{\sigma}}{Y_{\varphi}\left(\frac{\partial\bar{\sigma}}{\partial\sigma_{11}}+\frac{\partial\bar{\sigma}}{\partial\sigma_{22}}\right)}-1 \tag{16}$$

2.4. M-K Model

In the MK analysis, it is assumed that there is an undesired additional thinning due to the rolling operations, is perpendicular to the principal strain directions meaning that the angle ψ is equal to 0. The sheet is composed of the two different thick regions which are denoted by `a' and `b', respectively.

In the model initial imperfection factor is described as the ratio of the thickness in weak region "*b*" to nominal

region "*a*", $f_0 = \left(t_0^b / t_0^a\right)$ A biaxial load which causes to the development of strain increments is performed to the nominal area. Necking occurs when the effective strain in the groove area is 10 times of that in the safe area [23-26]. During the entire process, the force equilibrium equations at the groove direction must be satisfied as follow:

$$\begin{aligned} F_{nt}^a &= F_{nt}^b \\ F_{nn}^a &= F_{nn}^b \end{aligned} \tag{17}$$

Here F_{nn} and F_{nt} are forces in the normal and tangential directions in the groove. By introducing the stress state in these areas, Equation 17 could be rewritten as:

$$\begin{aligned} \sigma_{nt}^a \exp\left(\varepsilon_3^a\right) t_0^a &= \sigma_{nt}^b \exp\left(\varepsilon_3^b\right) t_0^b \\ \sigma_{nn}^a \exp\left(\varepsilon_3^a\right) t_0^a &= \sigma_{nn}^b \exp\left(\varepsilon_3^b\right) t_0^b \end{aligned} \tag{18}$$

where σ_{nn} and σ_{nt} are stress components in the ''n'' and ''t'' directions, t_0^a and t_0^b are initial thicknesses in the safe and groove regions, respectively. Imperfection factor, *f*, can be expressed as a function of the initial defect:

$$f = f_0 \exp(\varepsilon_3^b - \varepsilon_3^a) \tag{19}$$

In order to compute the stresses ($\sigma_{nn}^b, \sigma_{nt}^b, \sigma_{tt}^b$) and strain increments ($d\bar{\varepsilon}^b$) at the groove region, the Newton-Raphson method is applied to the following four equations generated:

$$\begin{aligned} F_1 &= \frac{d\varepsilon_{nn}^b \sigma_{nn}^b + d\varepsilon_{nt}^b \sigma_{nt}^b + d\varepsilon_{tt}^b \sigma_{tt}^b}{d\bar{\varepsilon}^b \bar{\sigma}_Y} - 1 = 0 \\ F_2 &= \frac{d\varepsilon_{tt}^b}{d\varepsilon_{tt}^a} - 1 = 0 \\ F_3 &= f\frac{\sigma_{nn}^b}{\sigma_{nn}^a} - 1 = 0 \\ F_4 &= f\frac{\sigma_{nt}^b}{\sigma_{nt}^a} - 1 = 0 \end{aligned} \tag{20}$$

In order to overcome the local minimum issue which is not the solution of the given equations, a backtracking algorithm is adopted to the Newton-Raphson method to find the suitable Newton step δx. The used Newton-Raphson method with backtracking algorithm is given below. The critical strain limit increment ($d\bar{\varepsilon}^b$) in the groove region is selected as ten times the normal region strain increment value ($d\bar{\varepsilon}^a$).

The convergence of Newton-Raphson method significantly depends on the selected initial values of the parameters. If the initial guesses of the parameters are not sufficiently close to the root, it is not possible to find the root of the generated nonlinear equation sets. In addition, the ratio between the strain increments in the normal and the groove regions may not reach to the selected value of 10 since the initial guess problem is the issue. To overcome this convergence problem, backtracking search algorithm can be adopted to Newton's method. The well-known Newton's method can be written in the following form:

$$F_i\left(x + \Delta x\right) = F_i\left(x\right) + \frac{\partial F_i}{\partial x_j}\Delta x_j + O\left(\Delta x^2\right), \text{ i=1,2,3,4}$$

By neglecting the terms of order $O\left(\Delta x^2\right)$ and setting $F_i\left(x+\Delta x\right)=0$, the increment form of the variable Δx, which is the direction of the Newton's step, can be calculated as follow:

$$\Delta x = -J^{-1}F$$

where J is the Jacobian matrix which is the partial derivative of the functions F to unknown parameter vector x. Then the solution vector is updated by adding the variable Δx with a λ multiplier.

$$x_{new} = x_{old} + \lambda \Delta x \ , \ \ 0 < \lambda \leq 1$$

where λ is the Newton step size and varies from 0 to 1. The purpose of the backtracking algorithm is to find the suitable λ multiplier which provides the rapid local convergence particularly for the close values of the strains to the necking situation. It is required to identify a criterion for which the convergence can be investigated. For this purpose, the function *g* which must decrease with the Newton's step is defined as a scalar multiplication of the target function ***F***.

$$g = F \cdot F$$

In every solution to function set ***F***, it is possible to find the local minima those are not the solution of ***F***. Therefore the strategy of finding λ has been used as follows:

$$\nabla g \cdot \Delta x = \left(F \cdot J\right).\left(-J^{-1} \cdot F\right) = -F \cdot F < 0$$

Due to the descent direction of the Newton's step, finding an acceptable step is guaranteed by backtracking along the Newton's step. At the initial of the algorithm, λ is selected as 1. In case the evaluated $H\left(x_{old}+\lambda\Delta x\right)$ function does not meet the acceptance criteria for the selected value of λ, it is required to calculate new one according to the used backtracking algorithm which is described as:

$$\Theta\left(\lambda\right) = H\left(x_{old}+\lambda\Delta x\right)$$

Therefore, it becomes:

$$\Theta'\left(\lambda\right) = \nabla H \cdot \Delta x$$

The algorithm starts with $\Theta\left(0\right)$ and $\Theta'\left(0\right)$ which are available at the initial evaluation of the target functions. The first step is always the Newton's step, $\lambda = 1$. If this step is not acceptable, $\Theta\left(1\right)$ is available as well. If $\Theta\left(\lambda\right)$ is considered as a quadratic function:

$$\Theta\left(\lambda\right) = \left[\Theta\left(1\right)-\Theta\left(0\right)-\Theta'\left(0\right)\right]\lambda^2 + \Theta'\left(0\right)\lambda + \Theta\left(0\right)$$

When the quadratic function's derivation is taken in terms of λ, it is possible to find the minimum as:

$$\lambda = -\frac{\Theta'\left(0\right)}{2\left[\Theta\left(1\right)-\Theta\left(0\right)-\Theta'\left(0\right)\right]}$$

On the second and subsequent backtracks, Θ is modeled as a cubic function of λ:

$$\Theta\left(\lambda\right) = p\lambda^3 + q\lambda^2 + \Theta'\left(0\right)\lambda + \Theta\left(0\right)$$

Using the previous value $\Theta(\lambda_1)$ and the second most recent value $\Theta(\lambda_2)$ provide two equations to obtain constants p and q:

$$\begin{bmatrix} p \\ q \end{bmatrix} = \frac{1}{\lambda_1 - \lambda_2} \begin{bmatrix} 1/\lambda_1^2 & -1/\lambda_2^2 \\ -\lambda_2/\lambda_1^2 & \lambda_1/\lambda_2^2 \end{bmatrix} \begin{bmatrix} \Theta(\lambda_1) - \Theta'(0)\lambda_1 - \Theta(0) \\ \Theta(\lambda_2) - \Theta'(0)\lambda_2 - \Theta(0) \end{bmatrix}$$

For the specific cases of p and q, the suitable λ values can be calculated as follow:

$$\lambda = \frac{-\Theta'(0)}{(2q)} \quad \text{if} \quad \text{p=0;}$$

$$\lambda = \begin{cases} \left[-q + \sqrt{q^2 - 3p\Theta'(0)}\right]/(3p), & q \le 0 \\ -\Theta'(0)/\left[q + \sqrt{q^2 - 3p\Theta'(0)}\right], & q > 0 \end{cases}$$

When the backtracking algorithm is integrated with the Newton-Raphson method, the divergence problem can be eliminated for the target functions ***F*** particularly for the neighboring strain values to failure.

3. RESULTS AND DISCUSSION

3.1. Comparison of the BBC Family Yield Criteria

In the following, all anisotropic yield criteria described above are applied to 304L stainless steel sheet in order to determine their applicability to the material. The performances of yield surfaces are checked via the comparison of the anisotropy and yield stress variations with respect to the orientation angle of the samples for different strain rates of 0.0016, 0.042 and 0.33 s^{-1}. In addition, three different methodologies used to determine the Lankford parameters are conducted to calculate the material parameters. One of these methods is based on the 15% prestrain value, the other one is the based on the 20% prestrain value and the last one is related to the slope of the deformations. As aforementioned before used, the calculated Lankford parameters are not the same for the different calculation methods.

Figure 4 depicts the results of different yield functions after calculating the yield stresses and anisotropy values with regards to the different orientations. As can be seen from the figures, BBC-2003 and BBC-2005 yield functions have almost the same prediction capability for all methodologies. In addition, they show the best agreement with the experimental results of the yield stress and anisotropy values. However, BBC-2000 and BBC-2008 are not successful on the predicting of the yield stress variation for the prescribed conditions. Besides that, the BBC-2000 is not capable of predicting the anisotropy variations particularly for 20% prestrain and the slope formulation form of the Lankford parameters.

The yield surfaces of the 304L stainless steel evaluated by using the considered yield criteria were also plotted in Figure 5. The models are evaluated for the different shear stresses σ_{12} = 0, 0.1, 0.2, 0.3, 0.4 and 0.5 in the normalized form.

The results revealed that there is no significant difference between the studied models except for BBC2000. The models behave similar at different strain rates. Therefore, in addition to Figure 5, the only predicted yield surfaces for altered methodologies are compared in Figure 6 for BBC2005 yield function at constant strain rate of 0.0016 s^{-1}. Although the surfaces are close to each other, the shear stress region is narrower for 15% prestrain value than those of the other methodologies. This difference is common in the biaxial region for all situations. Due to a similar behavior was obtained for other yield criteria, their results were not plotted in this paper. However; the material parameters for the studied models at different strain rates and methodologies are tabulated in Table 2.

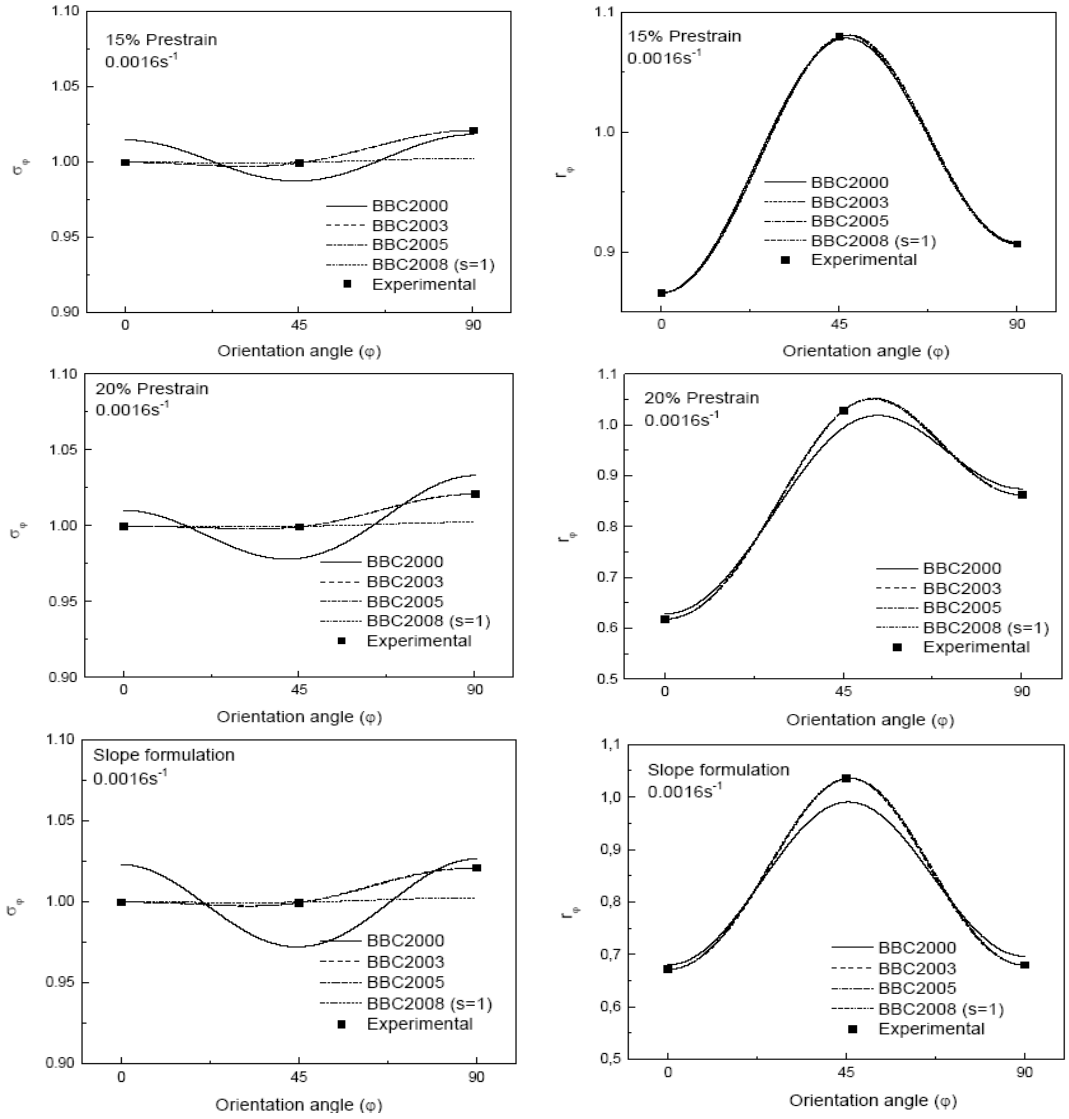

Figure 4. Comparison of different methodologies for calculating the anisotropies and yield stresses

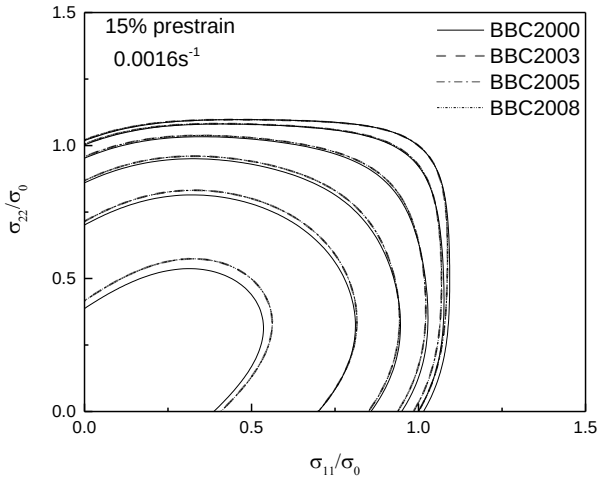

Figure 5. Comparison of the predicted yield surfaces for different shear stresses

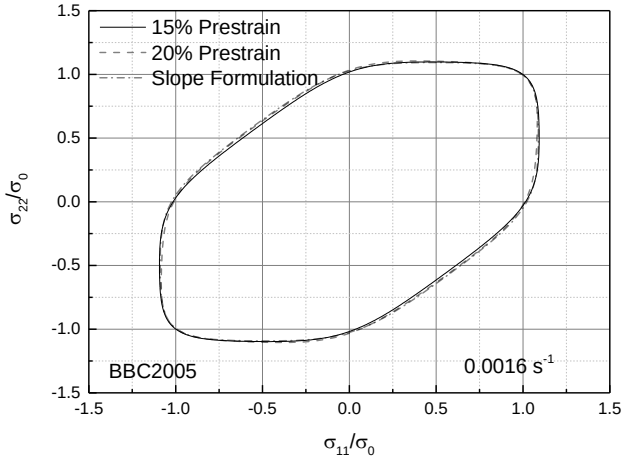

Figure 6. Comparison of the different methodology for BBC2005 yield function

Table 2. Material parameters for the BBC family yield criteria

		BBC2000							
Material Parameters		**a**	**b**	**c**	**M**	**N**	**P**	**Q**	**R**
15% Prestrain	**0.0016 0.042, 0.33 s^{-1}**	0.5016, 0.4168, 0.5167	0.8282, 0.8456, 0.8862	0.6704, 0.6269, 0.6692	0.6085, 0.5973, 0.6075	0.5989, 0.6159, 0.5185	0.7289, 0.7495, 0.6950	-0.7296, -0.7389, -0.7112	2.2995, 2.3360, 2.2417
20% Prestrain	**0.0016, 0.042, 0.33 s^{-1}**	0.5560, 0.4374, 0.5000	0.8235, 0.8360, 0.8836	0.6831, 0.6266, 0.6606	0.6359, 0.6248, 0.5699	0.5647, 0.5924, 0.5560	0.7065, 0.7427, 0.7247	-0.7182, -0.7442, -0.7241	2.2893, 2.3887, 2.2337
Slope Formulation	**0.0016, 0.042, 0.33 s^{-1}**	0.5746, 0.4343, 0.4902	0.8612, 0.8366, 0.8458	0.6771, 0.6262, 0.6302	0.5743, 0.6188, 0.6109	0.5697, 0.5991, 0.5750	0.7180, 0.7452, 0.7509	-0.7170, -0.7437, -0.7550	2.3805, 2.3791, 2.4538
		BBC2003							
Material Parameters		**a**	**M**	**N**	**P**	**Q**	**R**	**S**	**T**
15% Prestrain	**0.0016, 0.042, 0.33 s^{-1}**	0.6153, 0.7517, 0.9962	0.9487, 0.9002, 0.8308	0.9645, 0.8954, 0.9063	0.9707, 0.9092, 0.9293	0.9643, 0.8234, 0.8323	1.0244, 1.0943, 1.7309	1.0058, 1.0066, 1.7641	1.0392, 1.0400, 1.7783
20% Prestrain	**0.0016, 0.042, 0.33 s^{-1}**	0.7862, 0.9498, 0.7549	0.8896, 0.8449, 0.8992	0.9533, 0.8752, 0.9238	0.9676, 0.8971, 0.9372	0.9420, 0.7976, 0.8607	1.0632, 1.3090, -1.0779	1.0851, 1.2422, -1.0341	1.1146, 1.2722, 1.0549
Slope Formulation	**0.0016, 0.042, 0.33 s^{-1}**	0.6079, 0.8983, 0.8312	0.9516, 0.8579, 0.8763	0.9994, 0.8806, 0.9173	1.0049, 0.9005, 0.9340	0.9717, 0.8043, 0.8504	1.0004, 1.2047, 1.1162	0.9808, 1.1341, 1.0863	1.0337, 1.1639, 1.1054
		BBC2005							
Material Parameters		**a**	**b**	**L**	**M**	**N**	**P**	**Q**	**R**
15% Prestrain	**0.0016, 0.042, 0.33 s^{-1}**	0.4598, 0.1566, 0.2255	0.5230, 0.3381, 0.3783	0.5185, 0.6082, 0.6055	0.4919, 0.5476, 0.4984	0.5001, 0.5447, 0.5445	0.5033, 0.5530, 0.5591	0.4856, 0.5081, 0.4309	0.4645, 0.4153, 0.4308
20% Prestrain	**0.0016, 0.042, 0.33 s^{-1}**	0.4877, 0.1543, 0.2265	0.5093, 0.3431, 0.3753	0.5307, 0.6275, 0.5811,	0.4721, 0.5302, 0.5226	0.5059, 0.5492, 0.5369	0.5135, 0.5629, 0.5447	0.4479, 0.48011, 0.4850	0.4599, 0.4138, 0.4357
Slope Formulation	**0.0016, 0.042, 0.33 s^{-1}**	0.4828, 0.1558, 0.2267	0.5111, 0.3411, 0.3760	0.5146, 0.6223, 0.5881	0.4897, 0.5339, 0.5154	0.5142, 0.5480, 0.5395	0.5171, 0.5604, 0.5493	0.4535, 0.4873, 0.4703	0.4316, 0.4143, 0.4334
		BBC2008 s=1							
Material Parameters		l_1	l_2	m_1	m_2	m_3	n_1	n_2	n_3
15% Prestrain	**0.0016, 0.042, 0.33 s^{-1}**	0.5131, 0.5261, 0.5481	0.4868, 0.4736, 0.4512,	0.4949, 0.4711, 0.4929	0.4981, 0.4783, 0.5061	0.4947, 0.4326, 0.4526	0.4964, 0.5314, 0.4490	0.4752, 0.4438, 0.4499	0.5108, 0.5197, 0.5131
20% Prestrain	**0.0016, 0.042, 0.33 s^{-1}**	0.5291, 0.5417, 0.5264	0.4706, 0.4577, 0.4733	0.5044, 0.4741, 0.4863	0.5119, 0.4860, 0.4933	0.4984, 0.4317, 0.4529	0.4516, 0.5078, 0.4996	0.4638, 0.4458, 0.4525	0.5038, 0.5223, 0.5118
Slope Formulation	**0.0016, 0.042, 0.33 s^{-1}**	0.5123, 0.5379, 0.5327	0.4876, 0.4615, 0.4669	0.5120, 0.4737, 0.4887	0.5148, 0.4845, 0.4976	0.4978, 0.4323, 0.4529	0.4584, 0.5133, 0.4857	0.4365, 0.4448, 0.4507	0.5049, 0.5211, 0.5120

3.2. Prediction of FLD via M-K Model

3.2.1. Effects of Yield Function

In this study, the BBC family anisotropic yield criteria are implemented into the M-K model with the simple hardening curve formulation Power law ($\sigma = K\varepsilon^n$) and the results are illustrated in Figure 7. The groove orientation is assumed to be perpendicular to the rolling direction. For this situation, there is not any shear stress during the loading conditions. Additionally, in the governing algorithm, the strain increment in the safe region $d\bar{\varepsilon}_a$ is assumed as 10^{-4} and the initial imperfection is taken as 0.995. During the calculation of the imperfection with the strain increment, the derivative form of the imperfection function is used in Jacobian of the set of equations (Equation 20) which are used for the determination of the stress components and strain increments in the groove region. This approach leads to the decrease in the forming limit curve contrary to the functions without the derivative form of the imperfection.

In Makkouk et al. [27] study the experimental forming limit curve of the 304L stainless steel was determined for fracture and necking situation of the materials. In most cases, to increase the reliability of the FLD of the steels, approximately 10% offsetting procedure is performed to experimental results. In the study both situations are plotted in Figure 7 and compared with the model results.

The predicted FLDs via the studied BBC family yield criteria seem to be almost the same as the yield surfaces behave. Although the BBC2000 yield function has the overestimation for the biaxial region, the difference is not that much significant for all yield functions. When the model results are compared with the experiment, the prediction in plane strain condition is low for the necking situation. However, the models predict the plain strain condition overly close to the experiment. Furthermore, the other part of the FLDs does not show good agreement with the experimental results.

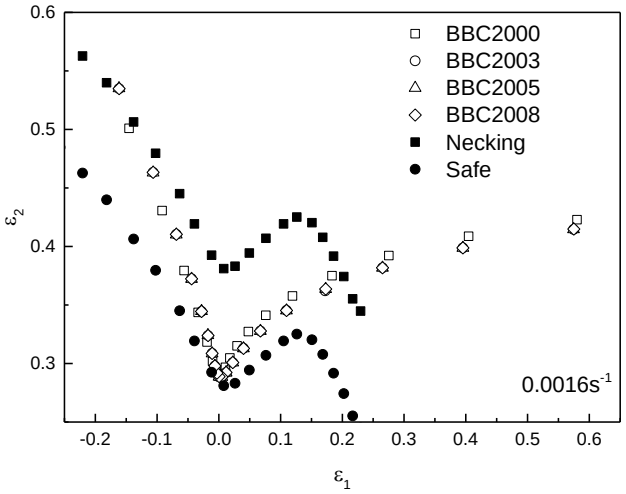

Figure 7. Comparison of the predicted FLDs via BBC family yield functions with the experimental data of 304L stainless steel

3.2.2. Effects of Methodology

In the literature, it is possible to find numerous studies about the effects of yield and hardening functions on the prediction capability of the developed instability criteria, particularly in M-K model. However; the comparison of the method used for the material parameters and their effects is lack. In Figure 8 the effects of the determination methodologies of the Lankford parameters on the FLD prediction are shown. The only BBC2005 anisotropic yield function is evaluated. It can be seen that the prediction results are different for three approaches. Particularly the difference is much clearer in the biaxial region. Although the calculations for 15% prestrain have higher limit strains in the biaxial region, these values are relatively smaller for the left hand side of the forming limit diagram. Moreover, slope formulation approach gives the minimum limit strains for the biaxial region.

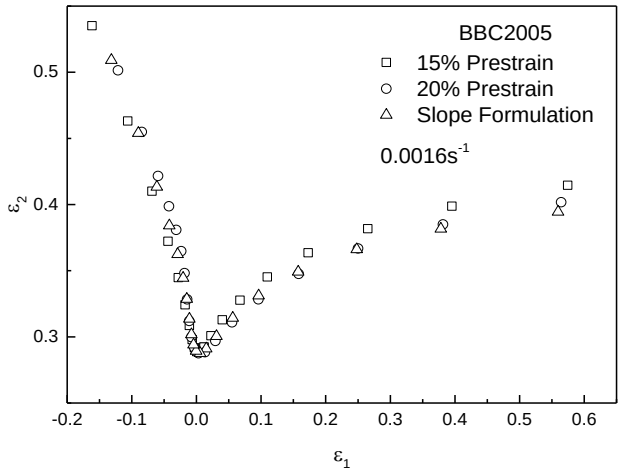

Figure 8. The effect of the methodology on the FLD prediction for the BBC2005 anisotropic yield function

3.2.3. Effects of Strain Rate

One of the most important parameters that affect the formability of the materials is the strain rate. When the deformation speed is increased during the forming operation, the formability tends to decrease. As aforementioned in the experiment section, the total elongation of the 304L stainless steels decreases from 66% to 57%. In this section the effects of the deformation speed on FLD are studied for BBC2005 and the results are depicted in Figure 9. Although the effect of deformation speed is not noteworthy for 0.0016 and 0.042 s^{-1}, the drop for 0.33 s^{-1} is remarkable particularly in the plane strain and biaxial deformation modes. Since the similar results are obtained from the other yield functions and methodologies, the results are not portrayed in the figure.

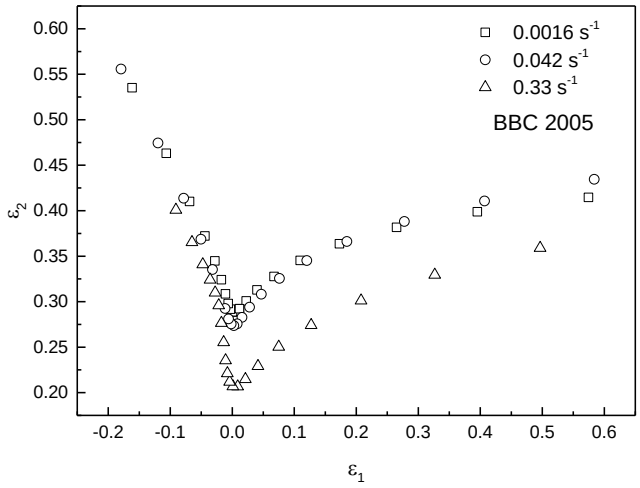

Figure 9. The effect deformation speeds on forming limit diagram

4. CONCLUSIONS

In this study, the formability characteristics of 304L stainless steel have been evaluated experimentally and numerically. In the experimental program, tensile tests have been performed at different strain rates. Furthermore, Lankford parameters have been calculated for different strain rates and methodologies. The Lankford parameters of the material have displayed difference for the selected cases and finally the effects of these variations on yield surfaces and forming limit diagram have been evaluated numerically. For this purpose, BBC family anisotropic yield functions and M-K instability criteria have been used in the calculations.

According to obtained results, in the view of the yield surfaces and FLD, there is no appreciable difference between BBC2003, BBC2005 and BBC2008 but BBC2000. The material parameters evaluated for different methodologies have given different responses for the forming limit diagrams and the slope formulation approach has proposed the lower formability characteristics in biaxial deformation modes.

REFERENCES

[1] KEELER S.P, BACKHOFEN W.A., "Plastic Instability and Fracture in Sheet Stretched over Rigid Punches", ASM Trans Quart, 56, 25, 1964.
[2] GOODWIN, G.M., "Application of Strain Analysis to Sheet Metal Forming in the Press Shop", SAE paper, No. 680093, 380, 1968.
[3] SWIFT, H.W., "Plastic Instability under Plane Stress", J Mech Phys Solids, 1, 1, 1952.
[4] HILL, R., "On Discontinuous Plastic States, with Special Reference to Localized Necking in Thin Sheets", J. Mech. Phys. Solids, 1, 19, 1952.
[5] HASHIGUCHI, K., PROTASOV A., "Localized Necking Analysis by the Subloading Surface Model with Tangential-Strain Rate and Anisotropy", Int. J. Plasticity, 20, 1909, 2004.
[6] BOUDEAU, N., GELIN, J.C., SALHI, S., "Computational Prediction of the Localized Necking in Sheet Forming Based on Microstructural Material Aspects", Comput Mater Sci., 11, 45, 1998.
[7] BRESSAN, J.D., WILLIAMS, J.A., "The use of a Shear Instability Criterion to Predict Local Necking in Sheet Metal Deformation", Int J Mech Sci., 25, 155, 1983.
[8] MARCINIAK, Z., KUCZYNSKI, K., "Limit Strains in the Processes of Stretch Forming Sheet Steel". J. Mech. Phys. Solids, 1, 609, 1967.
[9] HUTCHINSON, J.W., NEALE, K.W., Sheet Necking-II. Time Independent Behavior. In: Koistinen, DP, Wang NM, editors. Mechanics of Sheet Metal Forming. New York: Plenum Press, 1964.
[10] BANABIC, D., ARETZ, H., PARAIANU, L., JURCO, P., "Applications of Various Fold Modeling Approaches", Model Simul Mater Sci. Eng., 13, 759, 2005.
[11] BANABIC, D., ARETZ, H.D., COMSA, S., PARAIANU, L., "An Improved Analytical Description of Orthotropy in Metallic Sheets", Int J Plasticity, 21, 493, 2005.
[12] HORA, P., TONG, L., REISSNER J., "A Prediction Method for Ductile Sheet Metal Failure in Fe-Simulation", Proc. Numisheet'96 Conf., Dearborn, Michigan, 252, 1996.
[13] ARRIEUX, R., BRUNET, M., VACHER, P., NHAT, T.N., "A Method to Predict the Onset of Necking in Numerical Simulation of Deep Drawing Operations", CIRP Annals, 45, 255, 1996.
[14] SLOTA, J., SPIŠÁK, E., "Comparison of the Forming Limit Diagram (FLD) Models for Drawing Quality (DQ) Steel Sheets", Metalurgija, 44, 249, 2005.
[15] ASTM E8/E8M-11 Standard Test Methods for Tension Testing of Metallic Materials. West Conshohocken: American Society for Testing and Materials; 2004.
[16] TALONEN, J., NENONEN, P., PAPE, G., HÄNNINEN, H., "Effect of Strain Rate on the Strain-Induced $\gamma \rightarrow \alpha'$ Martensite Transformation and Mechanical Properties of Austenitic Stainless Steels", Metall Mater Trans A 36A: 421–32, 2005.
[17] CHUNG, K., AHN, K., YOO, H.D,, CHUNG, K.H., SEO, M.H., PARK, S.H., "Formability of TWIP (Twinning Induced Plasticity) Automotive Sheets", Int J Plasticity, 27, 52–81, 2011.
[18] BANABIC, D., KUWABARA, T., BALAN, T., COMSA, D.S., JULEAN, D., "Non -Quadratic Yield Criterion for Orthotropic Sheet Metals under Plane-Stress Conditions", Int. J. Mech. Sci., 45, 797-811, 2003.
[19] BARLAT, F., LIAN, J., "Plastic Behaviour and Stretchability of Sheet Metals (Part I): A Yield Function for Orthotropic Sheet under Plane Stress Conditions", Int J Plasticity, 5, 51–56, 1989.
[20] BANABIC, D., ARETZ, H., COMSA, D.S., PARAIANU, L., "An Improved Analytical Description Oforthotropy in Metallic Sheets", Int. J. Plasticity, 21, 493–512, 2005.
[21] BANABIC, D., COMSA, D.S., SESTER, M., SELIG, M., KUBLI, W., MATTIASSON, K., SIGVANT, M., "Influence of Constitutive Equations on the Accuracy of Prediction in Sheet Metal Forming Simulation", Proceeding of the Numisheet Conference, Interlaken, Switzerland, 37-42, 2008,
[22] COMSA, D.S., BANABIC, D., Plane-Stress Yield Criterion for Highly-Anisotropic Sheet Metals. In: Hora P (ed) Proceedings of the 7th International Conference and Workshop on Numerical Simulation of 3D Sheet Metal Forming Processes, NUMISHEET 2008, Interlaken, Switzerland, 43–8,2008.
[23] CAO, J., YAO, H., KARAFILLIS, A., BOYCE, M.C., "Prediction of Localized Thinning in Sheet Metal Using a General Anisotropic Yield Criterion", Int. J. Plasticity, 16, 1105–29, 2000.

[24] YAO, H., CAO, J., "Prediction of Forming Limit Curves Using an Anisotropic Yield Function Prestrain Induced Backstress". Int. J. Plasticity, 18, 1013–38, 2002.
[25] BUTUC, M.C., ROCHA, A.B., GRACIO, J.J., DUARTE, J.F., "A More General Model for Forming Limit Diagrams Prediction", J. Mater Process Technol., 125–126, 213–218, 2002.
[26] BUTUC, M.C., BANABIC, D., DA ROCHA, A.B., GRACIO, J.J., DUARTE, J.F., JURCO, P., COMSA, D.S., "The Performance of YLD96 and BBC2000 Yield Functions in Forming Limit Prediction", J. Mater Process Technol., 125–126: 281–286, 2002.
[27] MAKKOUK, R., BOURGEOIS, N., SERRI, J., BOLLE, B., MARTINY, M., TEACA, M., FERRON, G., "Experimental and Theoretical Analysis of the Limits to Ductility of Type 304 Stainless Steel Sheet", Eur. J. Mech. A-Solid, 27: 181–94, 2008.